(Final Project EN530.767, Spring 2018) Flow around cylinder at low and moderately high Reynolds numbers

Ghanesh Narasimhan, Hopkins ID: 33BF56

May 14, 2018

1 Introduction

The problem of flow around cylinder is considered. The objective of this project is to develop a flow solver that solves Navier-Stokes equations in cartesian coordinates and simulate the flow around cylinder by implementing simple immersed boundary methods like Volume penalization method or stair-step method. The flow should be simulated in an appropriate computational domain using fractional-step method for time-stepping. Reynolds number $Re = 150$ and other Re should be considered. The unsteady vortex shedding should be studied by comparing its shedding frequency with the values obtained in previous literatures. The contours of vorticity, pressure and velocities should be plotted and discussed.

2 Methodology

2.1 Governing equations

The governing equations for an incompressible fluid flowing around a cylinder are continuity and momentum equations:

$$\frac{\partial u_i}{\partial x_i} = 0, \tag{1}$$

$$\frac{\partial u_i}{\partial t} + \frac{\partial u_i u_j}{\partial x_j} + \frac{1}{\rho}\frac{\partial p}{\partial x_i} - \frac{\partial}{\partial x_j}\left(\nu \frac{\partial u_i}{\partial x_j}\right) + f_i = 0, \tag{2}$$

where $i = 1, 2$ such that $u_1 = u, u_2 = v, x_1 = x, x_2 = y$ and j is the repeated index. The term f_i represents the force on the fluid owing to the cylinder. These equations can be non-dimensionalized using the scalings

$$u_i^* = u_i/U,\ p^* = p/(\rho U^2),\ x_i^* = x_i/L,\ t^* = tL/U.$$

Using these scalings, the non-dimensional equations become

$$\frac{\partial u_i^*}{\partial x_i^*} = 0, \tag{3}$$

$$\frac{\partial u_i^*}{\partial t^*} + \frac{\partial u_i^* u_j^*}{\partial x_j^*} + \frac{\partial p^*}{\partial x_i^*} - \frac{\partial}{\partial x_j^*}\left(\frac{1}{Re}\frac{\partial u_i^*}{\partial x_j^*}\right) + f_i^* = 0, \tag{4}$$

where $Re = UL/\nu$ is the Reynolds number of the flow, U velocity scale is absorbed into a. The flow at the left boundary condition is chosen as the characteristic flow velocity such that $U = 1$. The

diameter of the cylinder is chosen as the charasteristic length scale to define the Reynolds number and the diameter L is set to 1. The $*$ in equations (3) and (4) will be dropped in the text for brevity. The equations (3) and (4) are the full conservative form of non-dimensionalized Navier-Stokes equations for an incompressible fluid with an external forcing term representing the force on fluid due to cylinder.

The scalar equations from (3) and (4) are

$$\frac{\partial u}{\partial x} + \frac{\partial v}{\partial y} = 0, \tag{5}$$

$$\frac{\partial u}{\partial t} + \frac{\partial u^2}{\partial x} + \frac{\partial uv}{\partial y} + \frac{\partial p}{\partial x} - \frac{1}{Re}\left(\frac{\partial^2 u}{\partial x^2} + \frac{\partial^2 u}{\partial y^2}\right) + f_1 = 0, \tag{6}$$

$$\frac{\partial v}{\partial t} + \frac{\partial uv}{\partial x} + \frac{\partial v^2}{\partial y} + \frac{\partial p}{\partial y} - \frac{1}{Re}\left(\frac{\partial^2 v}{\partial x^2} + \frac{\partial^2 v}{\partial y^2}\right) + f_2 = 0. \tag{7}$$

2.2 Volume penalization immersed boundary method

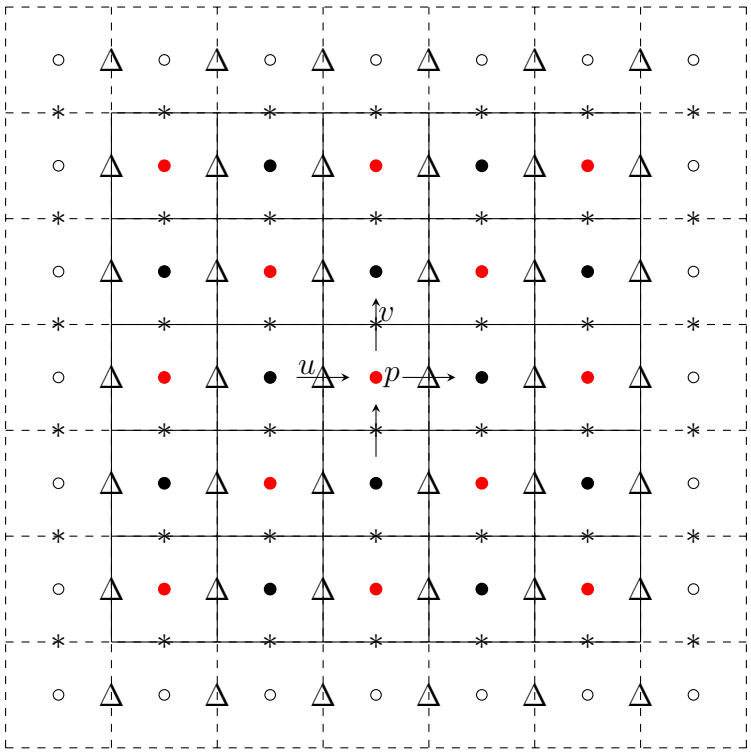

Figure 1: Staggered grid arrangement: p stored at cell centers (circles), u and v stored at cell faces Δ and $*$ respectively.

2.2.1 External forcing in volume penalization method

The flow around cylinder is implemented using Volume penalization immersed boundary method. In this method, the governing equations (5), (6) and (7) are solved simultaneously. The external forcing term f_i takes the form

$$f_i = a(x_i)(u_i - u_0), \tag{8}$$

where, u_i is the flow velocity and u_0 is the cylinder's velocity. A stationary cylinder is assumed and therefore $u_0 = 0$. The function $a(x_i, y_i) \sim 1/\Delta t$ and it is chosen such that it represents a cylinder of

diameter 1. Now, $a(x_i)$ is written as

$$a(x_i, y_i) = \frac{K(x_i - x_0, y_i - y_0)}{\Delta t}, \tag{9}$$

where x_0, y_0 coordinate is the desired location of the cylinder. Let's define the radius of the cylinder as $r_i = \sqrt{(x_i - x_0)^2 + (y_i - y_0)^2}$. Then, $K(x_i - x_0, y_i - y_0)$ is defined as

$$K(x_i - x_0, y_i - y_0) = \begin{cases} 10^8, & r_i < 0.5, \\ 0, & r_i \geq 1 \end{cases} \tag{10}$$

This definition of $K(x_i - x_0, y_i - y_0)$ ensures that the flow velocities within the cylinder are negligible when compared to the surrounding flow velocities.

2.3 Fractional step method

Consider a staggered grid arrangement as shown in figure 1. A first order fractional step method is used to solve the equations (5),(6) and (7). The convection and diffusion terms are discretized in time using a mixed Forward Euler and Backward Euler (FE+BE) scheme respectively. Second order central differencing is used for spatial discretization.

1. The fractional step method is implemented as follows:

$$\frac{u_i^* - u_i^n}{\Delta t} = -\left(\frac{\partial u_i u_j}{\partial x_j}\right)^n + \frac{1}{Re}\frac{\partial^2 u_i^*}{\partial x_j^2} - \frac{K}{\Delta t}u_i^*, \tag{11}$$

$$\frac{u_i^{n+1} - u_i^*}{\Delta t} = -\frac{\partial p^{n+1}}{\partial x_i}. \tag{12}$$

   Equation (11) is solved using point Gauss-Seidel method to obtain u_i^*. This predicted velocity is used in (12) to obtain pressure p^{n+1} by solving the following pressure Poisson equation obtained by taking divergence of (12):

$$\frac{\partial^2 p^{n+1}}{\partial x_i^2} = \frac{1}{\Delta t}\frac{\partial u_i^*}{\partial x_i}. \tag{13}$$

   This pressure Poisson equation is solved using Successive Over Relaxation method. The obtained p^{n+1} is substituted back in (12) to obtain u_i^{n+1} (velocity correction step),

$$u_i^{n+1} = u_i^* - \Delta t\frac{\partial p^{n+1}}{\partial x_i}. \tag{14}$$

2. Finite difference equations at the interior of the cell.

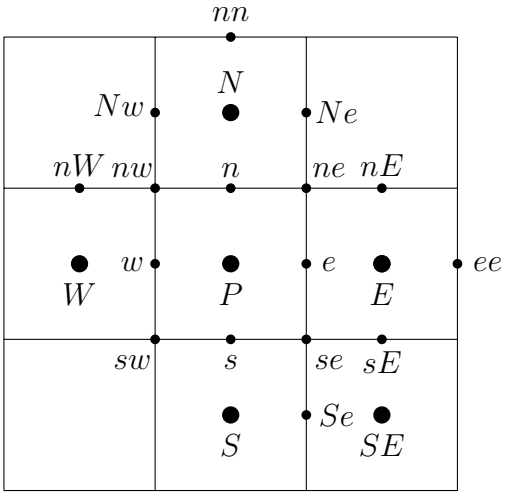

Figure 2: Interior cell

The discretized form of advection-diffusion equation (11) for the interior cell with center P are,

$$\frac{u_e^* - u_e^n}{\Delta t} = -\frac{(u_E^2)^n - (u_P^2)^n}{\Delta x} - \frac{(u_{ne}v_{ne})^n - (u_{se}v_{se})^n}{\Delta y} + \frac{1}{Re}\left(\frac{u_{ee}^* - 2u_e^* + u_w^*}{\Delta x^2} + \frac{u_{Ne}^* - 2u_e^* + u_{Se}^*}{\Delta y^2}\right) - \frac{K_u}{\Delta t}u_e^*, \tag{15}$$

$$\frac{v_n^* - v_n^n}{\Delta t} = -\frac{(v_N^2)^n - (v_P^2)^n}{\Delta y} - \frac{(u_{ne}v_{ne})^n - (u_{nw}v_{nw})^n}{\Delta x} + \frac{1}{Re}\left(\frac{v_{nE}^* - 2v_n^* + v_{nW}^*}{\Delta x^2} + \frac{v_{nn}^* - 2v_n^* + v_s^*}{\Delta y^2}\right) - \frac{K_v}{\Delta t}v_n^*, \tag{16}$$

where

$$u_{ne} = \frac{u_{Ne} + u_e}{2},\ v_{ne} = \frac{v_n + v_{nE}}{2},\ u_E = \frac{u_{ee} + u_e}{2},\ u_P = \frac{u_e + u_w}{2},$$
$$v_N = \frac{v_{nn} + v_n}{2},\ v_P = \frac{v_n + v_s}{2},\ u_{nw} = \frac{u_{Nw} + u_w}{2},\ v_{nw} = \frac{v_{nW} + v_n}{2}.$$

Equations (15) and (16) can be written as

$$u_e^*\left(1 + K_u + \frac{2\Delta t}{Re}\left(\frac{1}{\Delta x^2} + \frac{1}{\Delta y^2}\right)\right) - \frac{\Delta t}{Re}\left(\frac{u_{ee}^* + u_w^*}{\Delta x^2} + \frac{u_{Ne}^* + u_{Se}^*}{\Delta y^2}\right) = u_e^n + \Delta t\left(-\frac{(u_E^2)^n - (u_P^2)^n}{\Delta x} - \frac{(u_{ne}v_{ne})^n - (u_{se}v_{se})^n}{\Delta y}\right),$$

$$v_n^*\left(1 + K_v + \frac{2\Delta t}{Re}\left(\frac{1}{\Delta x^2} + \frac{1}{\Delta y^2}\right)\right) - \frac{\Delta t}{Re}\left(\frac{v_{nE}^* + v_{nW}^*}{\Delta x^2} + \frac{v_{nn}^* + v_s^*}{\Delta y^2}\right) = v_n^n + \Delta t\left(-\frac{(v_N^2)^n - (v_P^2)^n}{\Delta y} - \frac{(u_{ne}v_{ne})^n - (u_{nw}v_{nw})^n}{\Delta x}\right),$$

where K_u and K_v represent the function defined on u-staggered and v-staggered grids respectively. The pressure Poisson equation (13) is discretized as

$$\frac{p_E^{n+1} - 2p_P^{n+1} + p_W^{n+1}}{\Delta x^2} + \frac{p_N^{n+1} - 2p_P^{n+1} + p_S^{n+1}}{\Delta y^2} = \frac{1}{\Delta t}\left(\frac{u_e^* - u_w^*}{\Delta x} + \frac{v_n^* - v_s^*}{\Delta y}\right).$$

The velocity correction equation (14) is discretized as

$$u_e^{n+1} = u_e^* - \Delta t \left(\frac{p_E^{n+1} - p_P^{n+1}}{\Delta x} \right),$$
$$v_n^{n+1} = v_n^* - \Delta t \left(\frac{p_N^{n+1} - p_P^{n+1}}{\Delta y} \right).$$

3. Boundary conditions and mass flow correction:

   The following boundary conditions are implemented:

   - At the left boundary,
   $$u = 1, v = 0, \frac{\partial p}{\partial x} = 0,$$
   - At the top and bottom boundaries,
   $$\frac{\partial u}{\partial y} = 0, v = 0, \frac{\partial p}{\partial y} = 0,$$
   - At the right boundary,
   $$\frac{\partial u}{\partial x} = 0, \frac{\partial v}{\partial x} = 0, \frac{\partial p}{\partial x} = 0.$$

   Owing to the presence of cylinder inside the flow, the $\nabla \cdot \boldsymbol{u}$ would not be 0 in the computational domain. The mass flow correction is implemented such that the net flux

   $$\int_\Omega \boldsymbol{u} \cdot \boldsymbol{n} \, dS = 0 \tag{17}$$

   The influx mass is $m_{in} = \Sigma \, u_i \, dS$ and the outflux mass is $m_{out} = \Sigma \, u_i \, dS$. The net mass flux is $\Delta m = m_{in} - m_{out}$. Let L_y be the length of the right boundary which is discretized using say N_y number of grid points. Now, if Δm is not negligible such that $\Delta m > 0$ or $\Delta m < 0$, then the outflow velocity has to be corrected such that (17) is satisfied. The corrected velocity at the outer boundary is

   $$u_i = u_i + \frac{\Delta m}{Ly}, \tag{18}$$

   where $\Delta m / Ly$ represents the velocity correction associated with the change in fluxes at each cell of the outer boundary.

3 Results and discussion

Using the methodology described in the previous section, the flow around the cylinder is simulated in the domain of length $L_x = 10$ and height $L_y = 5$. The flow around cylinder is simulated for three Reynolds numbers: $Re = 150$, $Re = 100$ and $Re = 40$.

Firstly, the simulations are done in the domain without considering the cylinder with boundary conditions $u = 1, v = 0$ in the left boundary, free slip boundary condition on all other walls and Neumann boundary condition $\partial p / \partial n = 0$ for the pressure on all the boundaries. Without the cylinder, the flow inside the domain would be uniform and it is shown in figure 3.(a). The figure shows u velocity plotted at $t = 10$. The flow is uniform throughout the domain with a flow velocity 1. The pressure

Poisson (PPE) solver uses the convergence criteria $|\nabla \cdot u^*/\Delta - \nabla^2 p < 10^{-5}|$ and it is seen in figure 3(c) that the PPE solver converges to the criteria within 1000 iterations.

As a next step towards simulating flow around cylinder is to realise the solid body in the domain. The fuctions $K_u(x_i - x_0, y_i - y_0)$ and $K_v(x_i - x_0, y_i - y_0)$ are defined from (10) for $x_0 = 2$ and $y_0 = 2.5$ on the u and v-staggered grids. The cylinder is introduced at $t = 0$ in the presence of the uniform flow with $u = 1$. Hence, at $t = 0$, the domain consists of a uniform flow with cylinder as shown in figure 3 (b).

The length and height of the domain is resolved using 129 and 64 grid points such that the cylinder contains 13×13 points within it. Using this computational domain, the flow around cylinder is simulated for $Re = 40, 100, 150$. The simulation is run till an unsteady wake structure is formed and the time evolution of vorticity, pressure, velocities for each case are plotted and dicussed. The flow is simulated till $t = 200$ for $Re = 150, 100$ case and till $t = 150$ for $Re = 40$ case. The residue of the PPE solver at the last time step of each case is shown in figure 3(c). It is evident that the residue is below the convergence criteria and hence, the solution from the equations are converged solutions.

In figure 4, the time evolution of the vorticity and pressure for $Re - 150$ at different times are shown. It can be seen that a wake structure starts to form at $t \sim 5$ and it grows into a long structure ($t = 50$ plot). This long structure is steady in time briefly. At $t = 65$, undulations in the structure is seen which at long times $t \sim 100$ become unsteady where the vortex is shed periodically. The time evolution of corresponding pressure and velocities are shown in figures 4 and 5.

Now, $Re = 100$ is considered and the time evolution of vorticity is plotted in 6. Similar to the $Re = 150$ case, even here the wake structure is formed. It is steady for some time and starts to become unstable around $t \sim 95$ and becomes fully unsteady at $t \sim 145$. The onset of unsteady oscillations is delayed for $Re = 100$ when compared to $Re = 150$. This suggests that the vortex shedding would take much longer time for even smaller Reynolds numbers. The time evolution of corresponding pressure, velocities are shown in 6 and 7.

The wake structure behind $Re = 40$ case is always steady and never undergoes vortex shedding. The steady wake structure of the vorticity is shown in figure 8. The Re of the system is small and therefore the inertial forces is not strong enough to cause instabilities in the flow that lead to unsteady vortex shedding. Hence, we see a steady wake structure behind the cylinder in this low Re case.

The steady wake structure has a negative u velocity in almost all the cases. Hence, this wake has a recirculating flow pattern behind the cylinder. The flow reverses back to the cylinder because of the adverse pressure gradient. The pressure behind the cylinder is much smaller than the stagnation point in the front. Hence, the flow travels along the cylinder's surface. The pressure is minimum at the top and bottom surface of the cylinder while the pressure at the back of the cylinder is higher than the top and bottom points. Hence, the flow which reaches the top of the cylinder is subjected to an adverse pressure gradient and as a result the flow separates from the cylinder's surface. This adverse pressure gradient leads to reverse flow which is seen as blue contours in all the u velocity contour plots. This phenomenon is common to all Re in the steady wake phase of the flow.

The steady wake structure behind the cylinder for $Re = 40$ has a particular length scale associated with it. In figure 11(a) obtained from [1], the time evolution of the length scale of the vortex is plotted. It is evident that the lengthscale becomes steady beyond time $t \sim 15$ for $Re = 50$. A similar analysis is performed for the steady wake structure of the $Re = 40$ case simulation and plotted in 11 (b). The steady-state lengthscale of the vortex is ~ 4 which is same as the given in the literature. However, the time at which it becomes steady doesn't match exactly with the literature.

For large Re case, the inertial forces leads to instabilities in the steady wake structure. These instabilities grow in time and eventually start shedding vortices as shown in figures 4 and 6. The vortex sheds at a particular frequency. The velocity v plotted at $x = 3.44$ and $y = 2.5$ as a function of time

in the figure 10 shows the oscillatory nature of the vortex shedding. It is evident the amplitude of oscillations is high for $Re = 150$ than the $Re = 100$ case. The $Re = 40$ case doesn't shed any vortices and therefore there is no v velocity at this point. The frequency of oscillations are for the large Re cases are obtained by taking the Fourier transform of the v velocity oscillations. The frequency of vortex shedding for $Re = 150$ is 0.234 rad/s and $Re = 100$ is 0.22 rad/s. The ratio of vortex shedding frequency to inverse of advection timescale (D/U) is called Strouhal number (S)

$$S = \frac{\omega D}{U}, \tag{19}$$

where D and U are the characteristic length and velocity scales. Since $D = U = 1$, the vortex shedding frequency represents the Strouhal number of the flow. Figure 11(c), obtained from [2] gives the relation between Strouhal number and Reynolder number Re for flow around cylinder. From this plot, the literature suggests that for $Re = 100$ and $Re = 150$, the corresponding Strouhal numbers are $S = 0.16$ and $S = 0.18$ respectively. Hence, the numerically obtained vortex shedding frequency doesn't match exactly with the literature. However, the qualitative picture of the vortex shedding is captured. A different immersed boundary method like the Ghost cell method where the cylinder would be treated as a boundary instead of a forcing term may be required to accurately capture the physics.

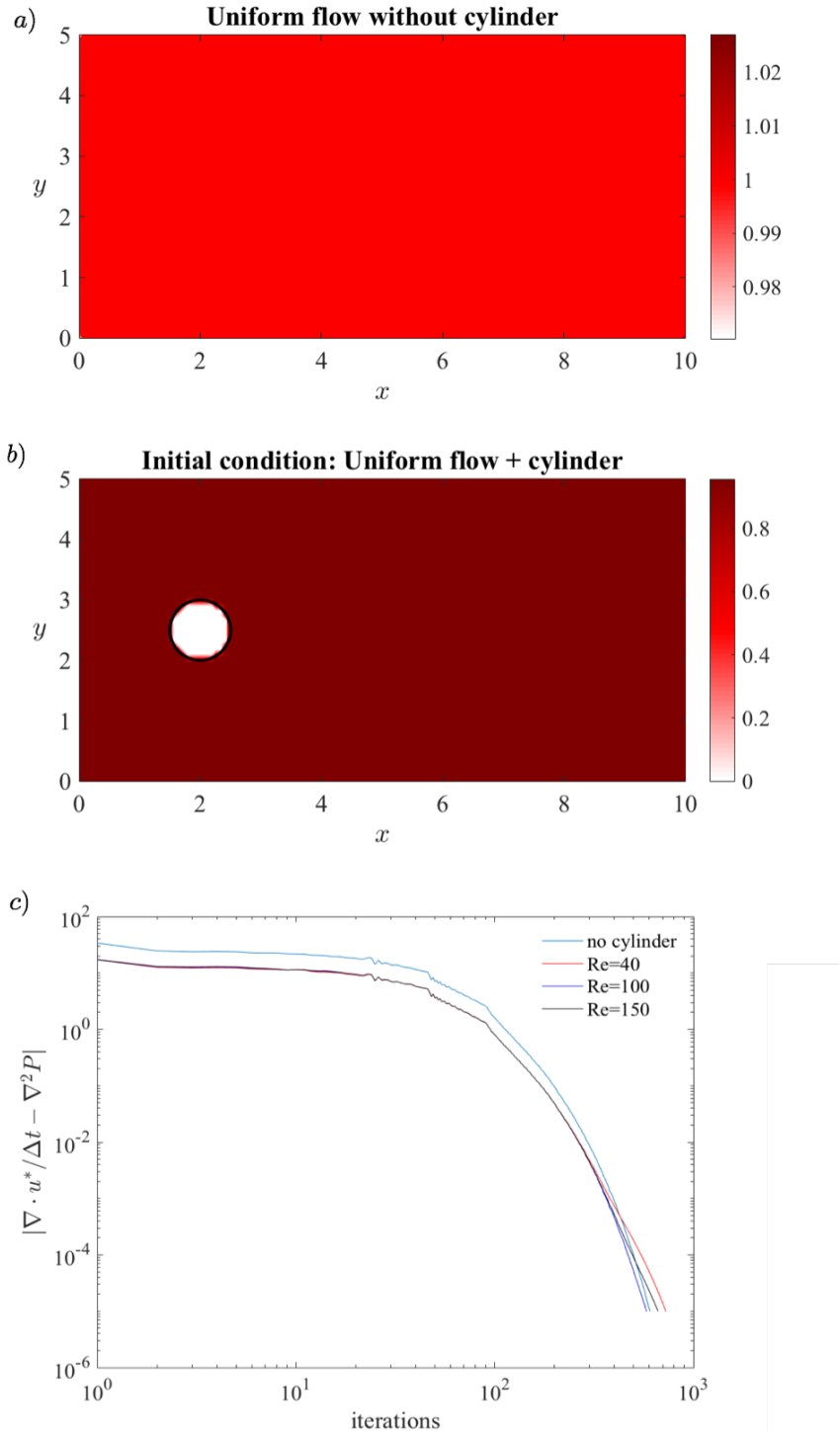

Figure 3: Contours of (a) uniform flow without cylinder, (b) flow with cylinder and (c) residue of pressure Poisson solver

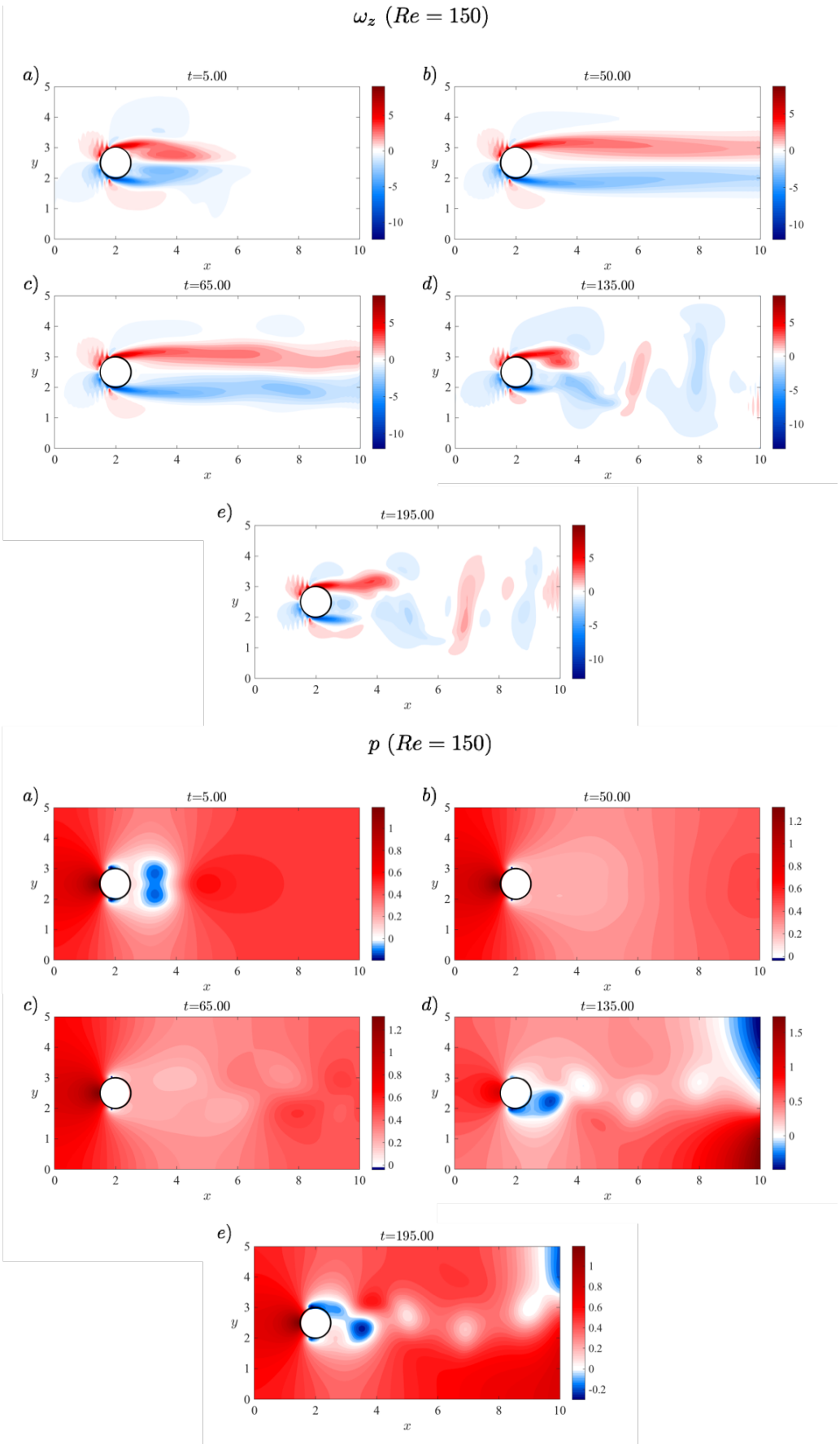

Figure 4: ω_z and p contours at different times for $Re = 150$

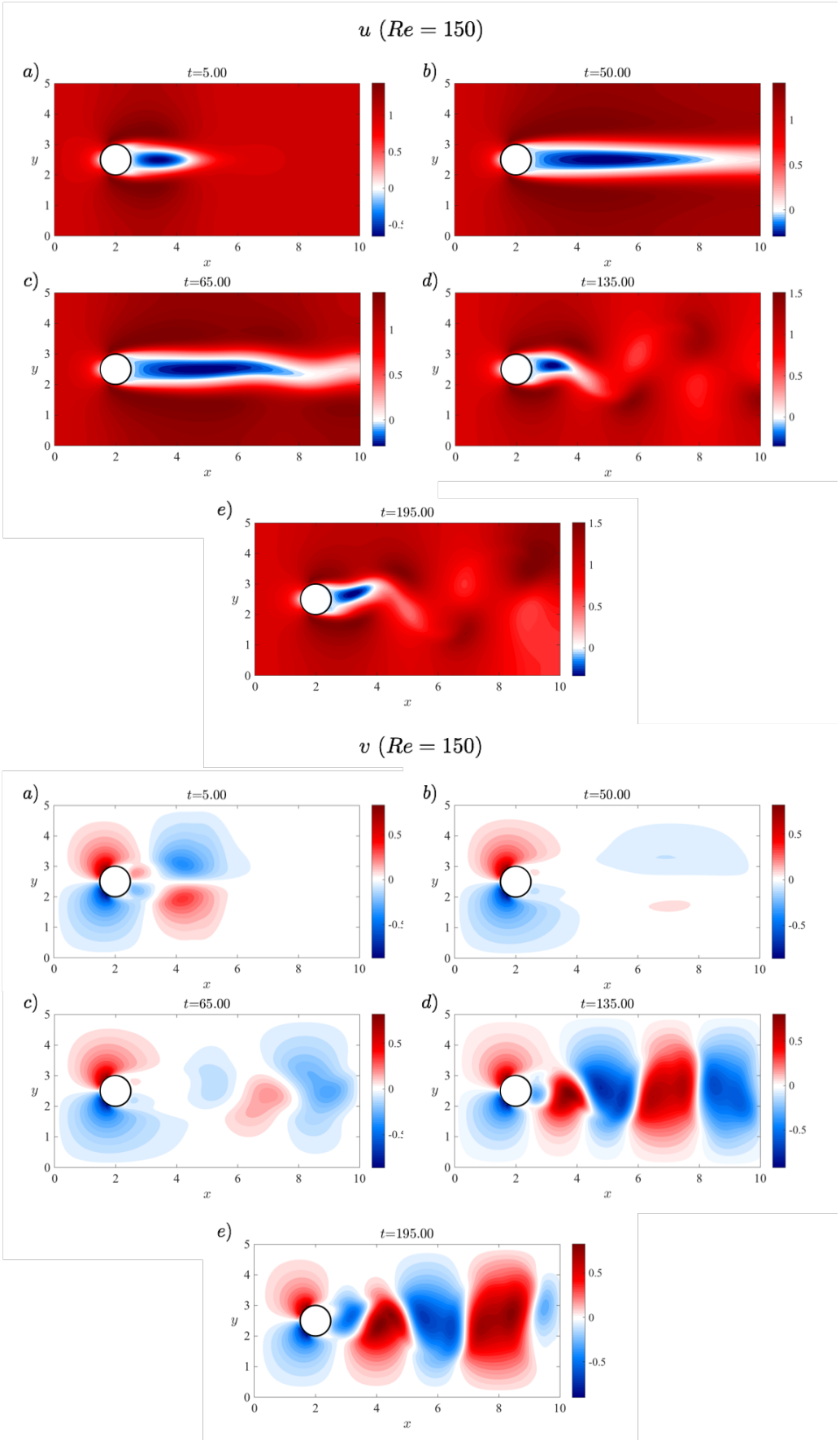

Figure 5: u and v contours at different times for $Re = 150$

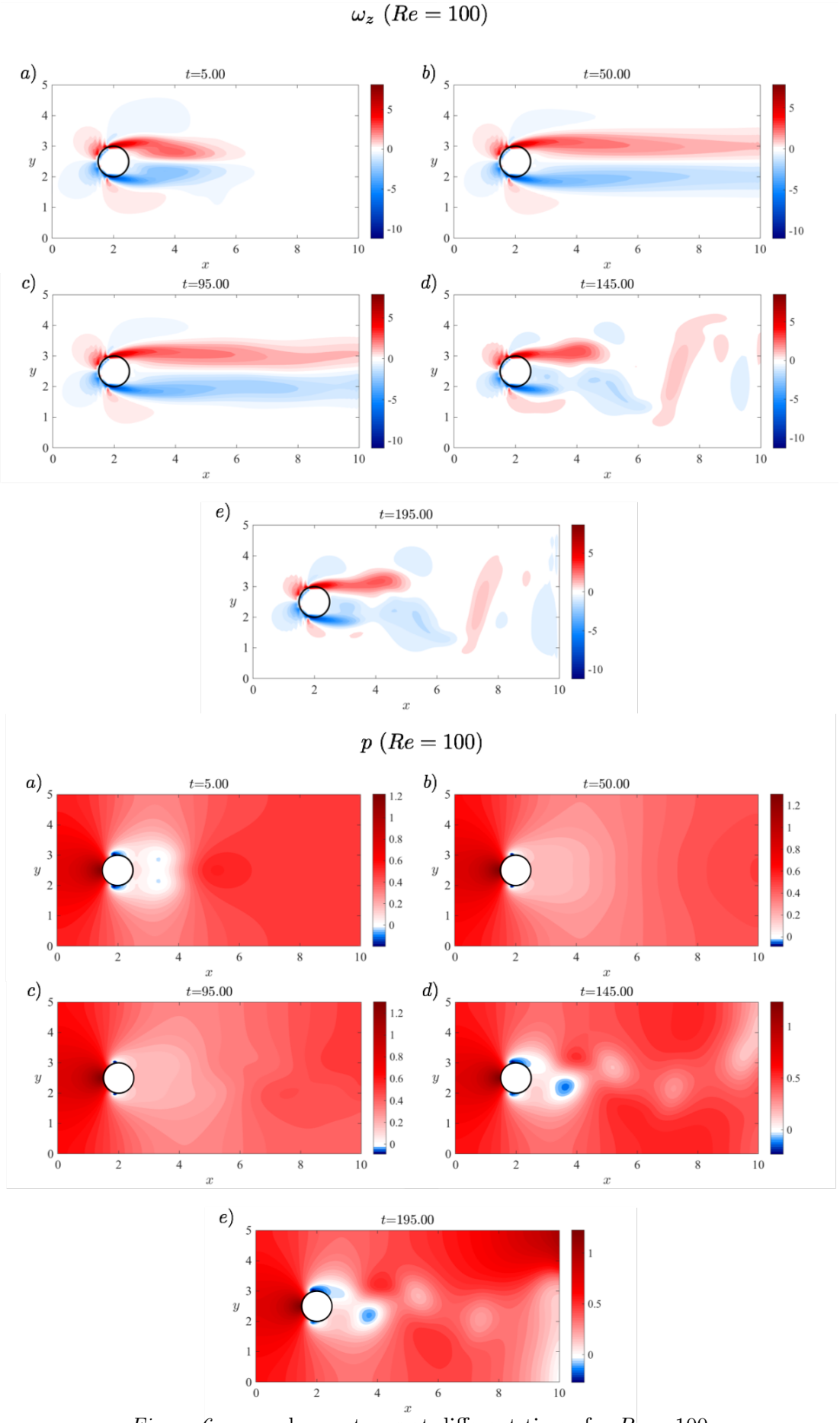

Figure 6: ω_z and p contours at different times for $Re = 100$

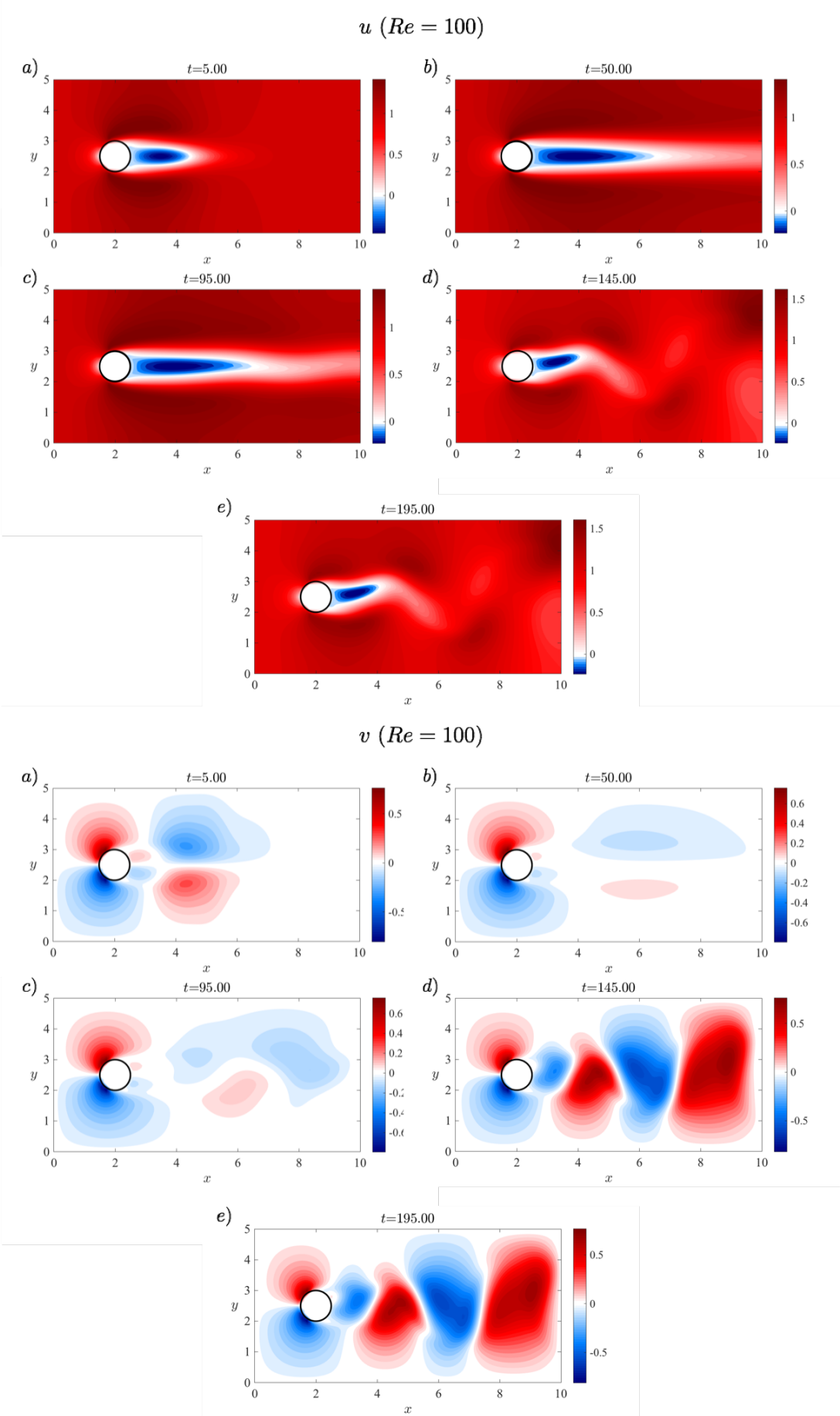

Figure 7: u and v contours at different times for $Re = 100$

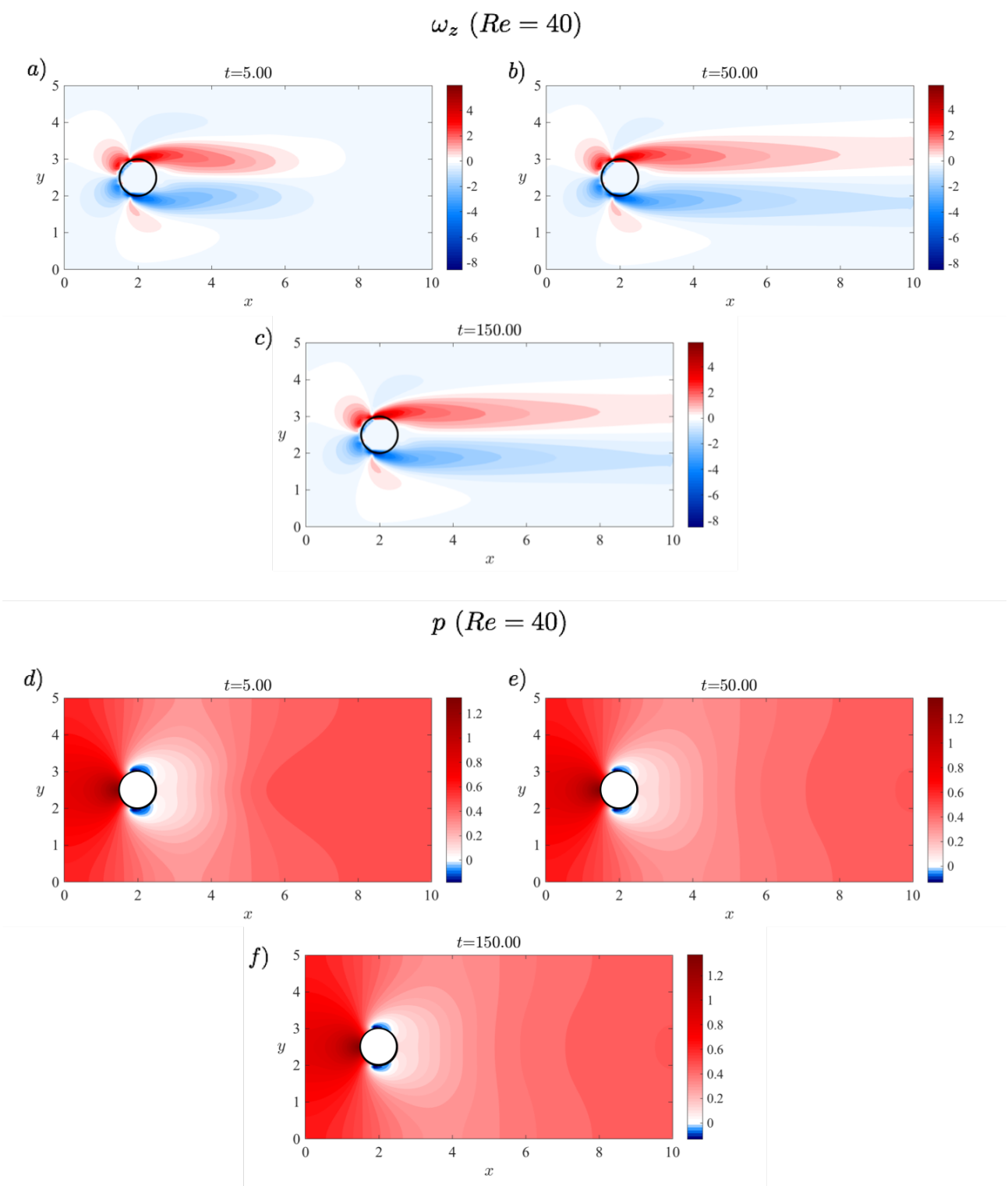

Figure 8: ω_z and p contours at different times for $Re = 40$

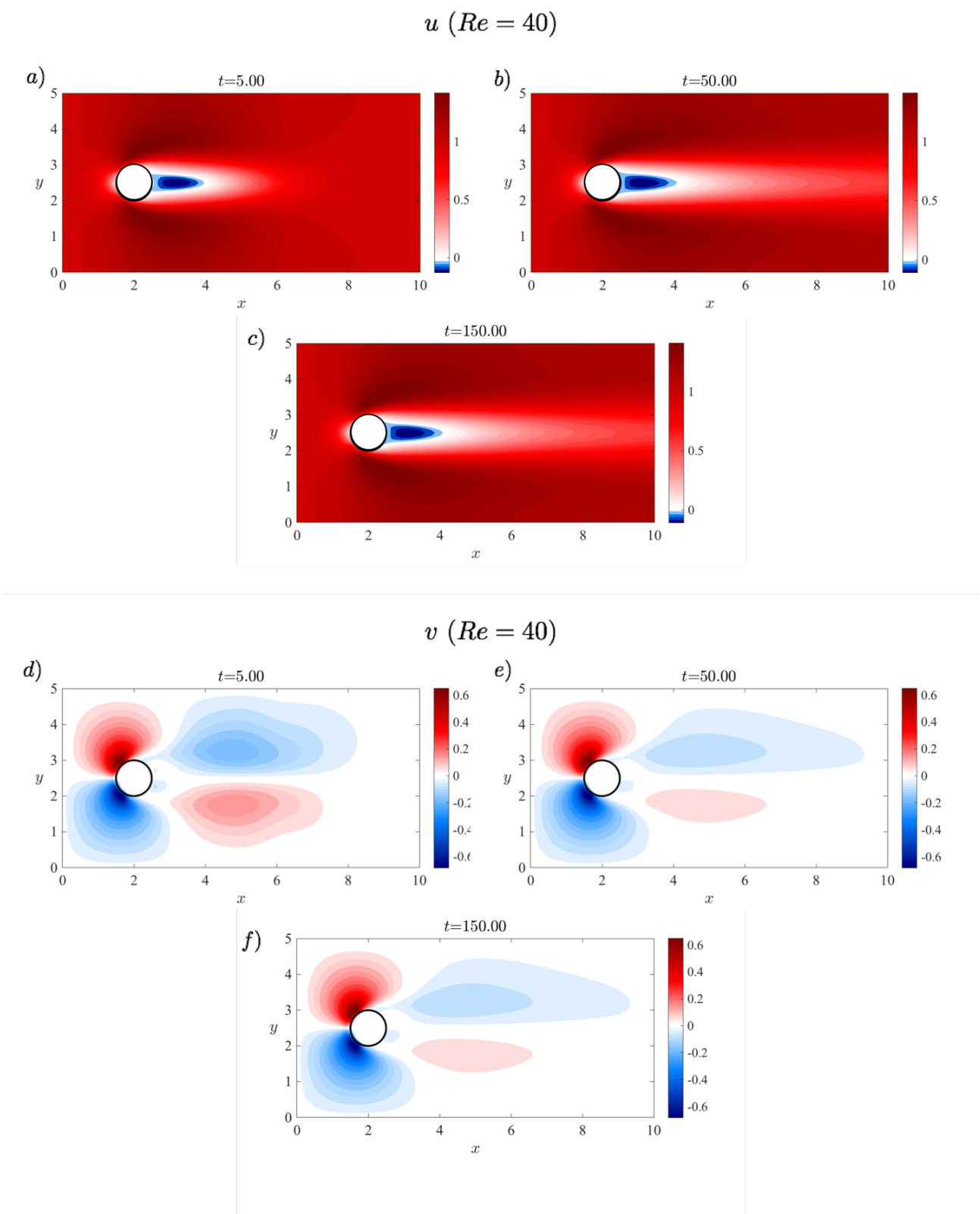

Figure 9: u and v contours at different times for $Re = 40$

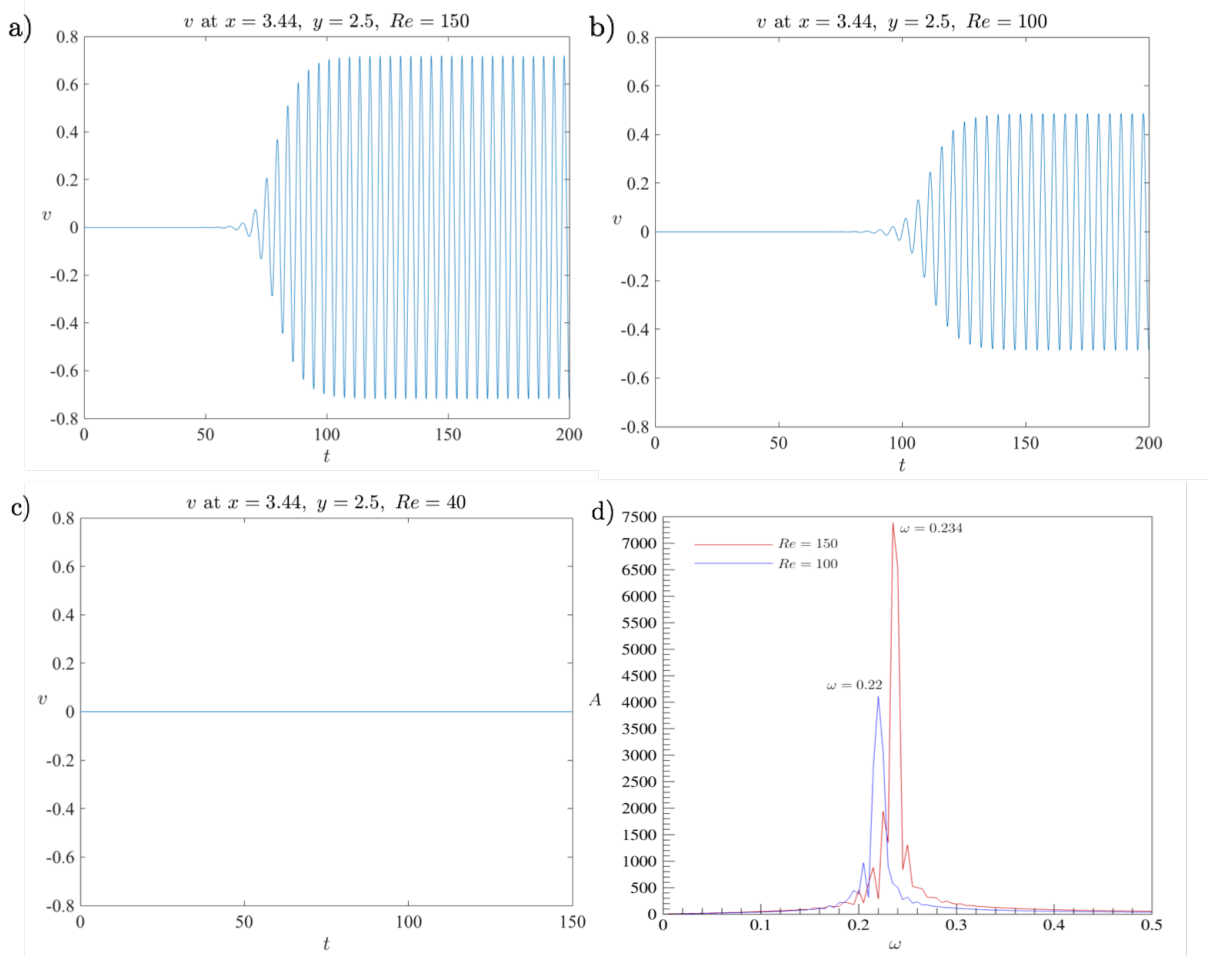

Figure 10: v at $x = 3.44, y = 2.5$ for a) $Re = 150$, b) $Re = 100$, c) $Re = 40$ and d) vortex shedding frequency for $Re = 150$ (red) and $Re = 100$ (blue).

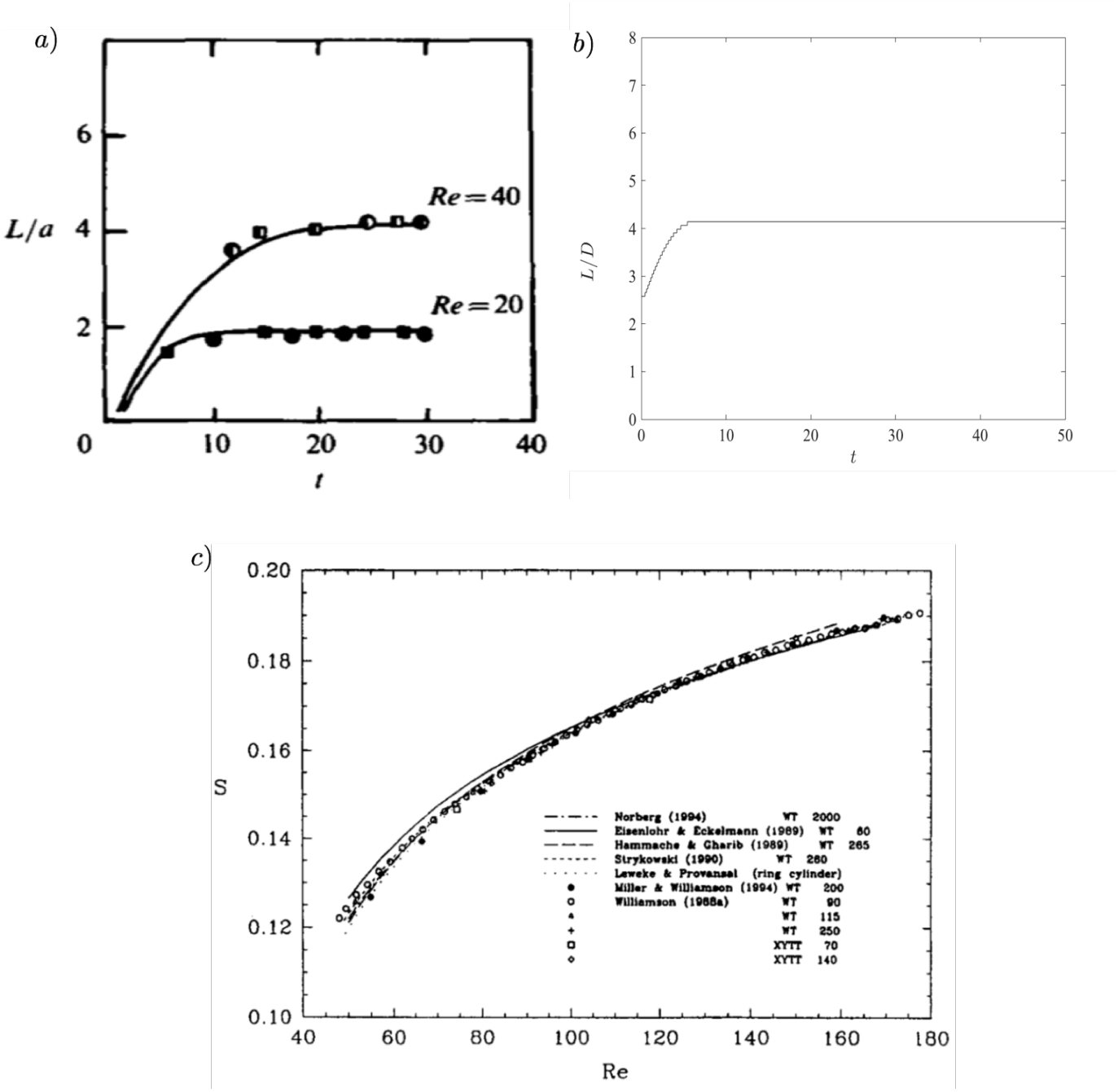

Figure 11: Reference value for steady state recirculation bubble length vs time in (a) for $Re = 40$ and $Re = 20$, computed recirculation bubble length for $Re = 40$ case in (b) and Strouhal number (S) vs Reynolds number (Re) relation for flow around cylinder.

4 Conclusion

A flow solver has been developed that solves the flow around cylinder in a cartesian grid. Volume penalization is used to implement the cylinder inside the flow. Simulations were preformed for $Re = 40, 100, 150$ cases on a 129×65 grid. The $Re = 40$ case has a steady wake structure behind the cylinder and doesn't undergo transition to the vortex shedding phase. The cases with $Re = 100, 150$ sheds vortices at long times and the vortex shedding frequencies are computed and compared with literature. The Strouhal number which represents the shedding frequency for $Re = 100$ and $Re = 150$ obtained

from the flow simulations are 0.22 and 0.234 respectively. These values doesn't exactly agree with the values reported in the literature [2]. It is proposed that the Volume penalization method that simulates the cylinder by introducing a forcing term in the Navier-Stokes equation might not capture the physics accurately. An accurate treatment of the cylinder boundary is required which can be achieved by implementing the Ghost cell based immersed boundary method. Alternatively, the volume penalization method can give accurate results if the cylinder is resolved using more number of points. Hence, a large computational grid might be required for the currently implemented immersed boundary method. The lengthscale of the recirculating bubble (steady wake structure) is also computed for the $Re = 40$ case and compared with the literature [1]. It is found that the wake length is ~ 4 which is the value reported in the literature. However, the time taken for the wake structure to become steady is different from the literature.

5 References

1. Braza et al 1986 Numerical study and physical analysis of the pressure and velocity fields in the near wake of a cylinder. J. Fluid Mech. 165, 79-130.

2. Williamson C. H. K. 1996 Vortex dynamics in the cylinder wake. Annu. Rev. Fluid. Mech. 28, 477-539

3. Class notes